Chapter 1

DYNAMICS & CONTROL OF JETS IN CROSSFLOW

Direct numerical simulations \mathscr{C} experiments

Peter N. Blossey
University of Washington

Satish Narayanan United Technologies Research Center

Thomas R. Bewley
University of California, San Diego

Abstract

The structure of a jet in crossflow and its mixing have been studied through detailed direct simulations, and the findings were verified by experiments. Using a newly developed pseudo-spectral code, simulations have been performed both with and without sinusoidal forcing at Strouhal numbers in the range $St_d = fU_j/d = 0.1$ –0.64. Based on the simulation results, which show substantial entrainment and mixing enhancements with lower frequency forcing, experiments have been performed for unforced and forced jets with jet Strouhal numbers up to $St_d = 0.2$. The simulations and experiments indicate that forcing at the lower end of the frequency range considered in the numerical results, namely $St_d = 0.1$ –0.26, is most effective for increased mixing and entrainment. Finally, we assess the benefits of the controlled flow states using a variety of time-averaged and unsteady mixing metrics.

Keywords: Jet in crossflow, transverse jet, forced jet.

Introduction

The jet in crossflow has wide application in industrial and environmental flows such as dilution jets in combustors and smokestacks in the

atmosphere. Mixing is central to these flows for cooling or reaction in combustors and for pollutant dispersion in the atmosphere.

In a jet in crossflow (also called a transverse jet), fluid emerges from an orifice at a large angle into a stream. The shear layer along the front (or upstream) edge of the jet develops oscillations which roll up into large pockets of jet fluid and travel along the upper edge of the jet, contributing to a high degree of intermittency there. As the trajectory of the jet bends to follow the crossflow direction, a counter-rotating vortex pair (CVP) forms and results in further entrainment of crossflow fluid.¹

The forcing of jets exhausting into quiescent fluid can have a substantial impact on the structure and mixing of the jet. Optimal forcing frequencies for increased mixing (explored experimentally) are claimed to be in the range $St_d=0.2$ –0.4 (Crow and Champagne, 1971; Vermeulen et al., 1992). Unsteadily forced jets in crossflow have also received attention in recent experimental and computational studies (Vermeulen et al., 1990; M'Closkey et al., 2001; Eroglu and Breidenthal, 2001). Our study combines direct numerical simulations of forced jets in crossflow with a preliminary experimental investigation of these flows in an attempt to determine both the most excitable and the most "beneficial" forcing frequencies. (Note that these two frequencies may not coincide.) To this end, the effect of sinusoidal forcing on mixing by the jet in crossflow is evaluated over a wide control parameter range.

1. Computational & Experimental Setup

Computational Setting. The jet in crossflow is simulated in a periodic channel flow geometry. The Navier–Stokes equations are solved without modeling (direct numerical simulation) and are discretized with Fourier modes in the wall-parallel directions and finite differences in the wall-normal direction. An advection-diffusion equation is solved to compute the evolution of a conserved, passive scalar field. Due to the periodic boundary conditions in the streamwise/crossflow direction, a fringe region is added near the exit of the channel (the last 30% of the domain) to remove fluctuations from the outgoing velocity and scalar fields and to provide the desired inflow boundary conditions. These techniques are commonly used in simulations of spatially-evolving disturbances in transitional boundary layers (Nordström et al., 1999). A

In addition to the jet shear layer and the CVP, two other structures — upright wake vortices and a horseshoe/necklace vortex — can sometimes be seen in the jet in crossflow for particular values of the Reynolds number and the ratio of jet exit velocity to that of the crossflow. Figure 29 in (Kelso et al., 1996) maps out the parameter values where the different structures may be expected to appear.

hybrid implicit-explicit Crank-Nicolson, Runge-Kutta scheme for time integration allows for the implicit treatment of the wall-normal convective and viscous terms, relieving the severe viscous and CFL time step restrictions imposed by the highly refined mesh near the wall and the flow of jet fluid across it. The scalar discretization employs upwinding (Leonard, 1988) in the wall-normal direction and filtering in the wallparallel directions to limit the appearance of non-physical oscillations in the scalar field due to the sharp gradients near the jet exit. The jet inflow into the simulation domain is imposed as a velocity boundary condition on the bottom wall of the channel with a inflow velocity profile defined as $v_i(r) = U_i \exp(-(2r/d)^8)$. This profile is then filtered to prevent the excitation of high frequencies which would appear as ringing in the velocity field, while still maintaining a near top hat profile typical for dilution jets in combustion applications. The imposition of the jet inflow as a boundary condition neglects the boundary layer details in the pipe flow leading to the jet exit. While separation in the pipe flow might significantly influence the dynamics of the emerging jet, (Kelso et al., 1996) observed that the flow in the pipe does not separate for velocity ratios R > 6 (R = 6 in these simulations).

The relevant parameters in the simulation are the domain size $25d \times 12d \times 10d$ and resolution $256 \times 120 \times 96$ (de-aliased) in the streamwise, wall-normal and spanwise directions, respectively; the jet Reynolds number $(Re_j = U_j d/\nu = 3000)$; the jet velocity ratio $(R = U_j/U_{\infty} = 6)$ and the forcing amplitude (F = 0.2), see equation 1.1). The range of forcing frequencies is $St_d = fd/U_j = 0.1$ –0.64. The jet velocity profile:

$$\mathbf{u}_{\text{wall}}(x,z) = [1 + F \sin(2\pi \ St_d \ t)] \ v_j(x,z) \ \mathbf{e}_2$$
 (1.1)

is modulated so that only the amplitude, not the shape, of the velocity profile changes with forcing.

Experimental Setting. Cold, non-reacting sub-scale experiments of unforced and forced jets in crossflow with a velocity ratio of 6 (as in the simulations) have also been conducted. The Reynolds number based on channel height was 27000, higher than in the simulations, but the jet Reynolds number of 5000 is similar to that used in the simulations. A mechanical actuator (a spinning valve) is used to modulate the jet at several frequencies in the range predicted as effective for mixing by the simulations ($St_d = 0.1\text{--}0.26$). The mechanical design and performance of this actuator are described in (Anderson et al., 2001). Mixing and entrainment are evaluated by flow visualization and quantitative measurements of the velocity field using TSI single hot-film probes.

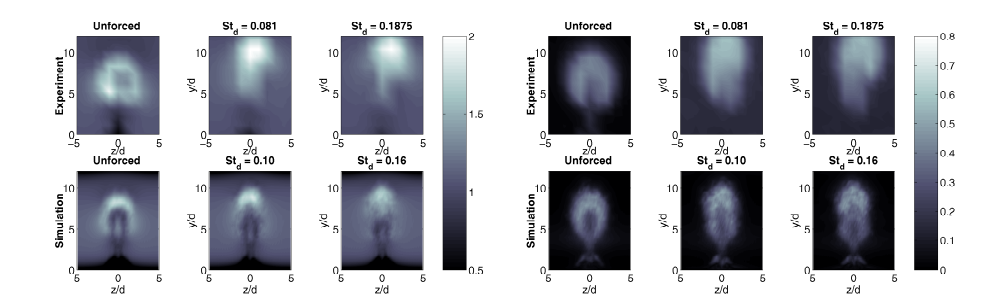


Figure 1.1. Comparison of the mean (left) and rms (right) profiles of the resultant velocity $u_{res} = (u^2 + v^2)^{1/2}$ at x/d = 4 in experiments (top) and simulations (bottom).

The experiments have been conducted in two phases. The first phase explored the "excitable" dynamics in the flow field, via unsteady forcing of the jet emanating into the crossflow over a wide range of frequencies (for a fixed amplitude). The response of the flow has been evaluated using velocity spectra from the hot film probe positioned at various locations both within and outside the jet as it emerges and bends into the crossflow. Forcing of the jet at high frequencies (namely, $St_d > 0.2$) results in an amplified flow response close to the jet orifice with diminishing response downstream, while low frequency forcing $(0.08 < St_d < 0.2)$ is observed to produce a response farther downstream that has higher amplification. Note that the jet in crossflow region beyond the first 3-5 jet diameters is of particular interest for mixing enhancement. This first phase of experiments (aimed at the identification of "excitable dynamics") have been followed by the second phase of proof-of-concept, open-loop control experiments to verify and validate the ideas proposed using the direct numerical simulations. The experimental results, including time-averaged surveys of the scalar and velocity fields and flow visualizations, will be described elsewhere (Narayanan et al., 2002).

2. Results

The ability of the simulations to capture the features of the jet in crossflow is limited to some degree by their resolution and Reynolds number, but they should be expected to capture some of the large-scale features of jets in crossflow measured experimentally at higher Reynolds numbers. The experiments measured the mean and fluctuating velocity using hot film probes parallel to the crossflow and wall-normal directions. These probes therefore measured the velocity $u_{res} = (u^2 + v^2)^{1/2}$, the resultant of the velocities in the streamwise and wall-normal directions (u and v, respectively). These quantities were computed in the simulations

and are displayed on matched non-dimensional scales with the experimental measurements in figure 1.1. The resultant velocities and fluctuations from the simulations compare reasonably well to those from the experiments considering the differences in the jet velocity profile (thicker shear layers in the simulations), the level of turbulence in the emerging jet (zero in the simulations/non-zero in the experiments), the Reynolds number (lower in the simulations), and the artificially-imposed periodic spanwise boundary conditions at $z=\pm 5d$. The forcing levels employed in the experiments are also much higher than those in the simulations. A nearly fully modulated jet is used in the experiments whereas only a partially modulated jet is used in the simulations. The results from the experiments and simulations match closely for the unforced jet, with similar penetration, spreading and magnitude. The forced jets show less penetration, spreading and velocity magnitude in the simulations than in the experiments. The stronger forcing and thinner shear layers in the experiments may lead to larger growth rates for modes in the shear layer and consequently to a larger response to the forcing. Further validation for the simulations comes from the mean concentration profile at x/d =5 in the unforced jet, which corresponds well to that measured by (Smith and Mungal, 1998) for a velocity ratio of R=5.

The structures in the jet shear layer and the counter-rotating vortex pair (CVP) can be seen clearly in the simulations of unforced jet in crossflow. The jet emerges into the crossflow, bends to follow the crossflow and impinges on the upper wall of the channel just downstream of x/d =10. Judging by the trajectory of the jet, the near field of the simulations (up to approximately x/d=6) is relatively unaffected by the presence of the channel's upper wall. The mean and fluctuating scalar fields for the unforced jet and the jet forced at $St_d = 0.16$ and 0.26 are shown in figure 1.2. These non-dimensional forcing frequencies were chosen after a survey of the intrinsic dynamics of the jet in crossflow (similar to that in experiments). Surveys of the velocity spectra along the jet trajectory as it bends into the crossflow reveals broadband spectral peaks surrounding $0.3 < St_d < 0.4$ near the jet exit associated with coherent, azimuthal-vorticity-dominated shear layer structures. However, farther downstream (where most of the vorticity dynamics are confined to a counter-rotating vortex pair with predominantly streamwise vorticity) lower frequency activity around $0.1 < St_d < 0.2$ is noted. Although the counter-rotating vortex pair appears symmetric in time-averaged images of the velocity and vorticity fields, the downstream structures are instantaneously far from symmetric and are highly unsteady (influenced strongly by the unsteady vortex dynamics occurring on the upstream edge of the jet). The complex, asymmetric counter-rotating structure

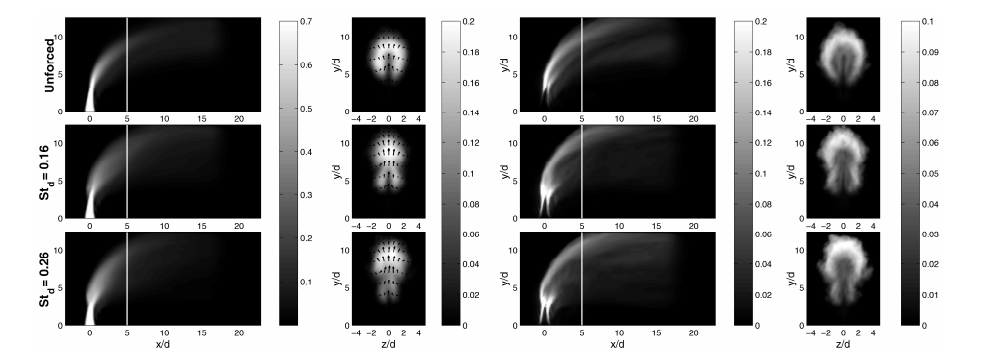


Figure 1.2. Mean (left) and rms (right) scalar profiles from direct simulation of an unforced jet in crossflow (top) and two forced cases at $St_d=0.16$ (middle) and $St_d=0.26$ (bottom). Each row shows an x-y slice (parallel to the crossflow direction) through the jet centerline and a y-z slice at x/d=5 (perpendicular to the crossflow direction) whose locations is marked by a vertical line in the x-y slice.

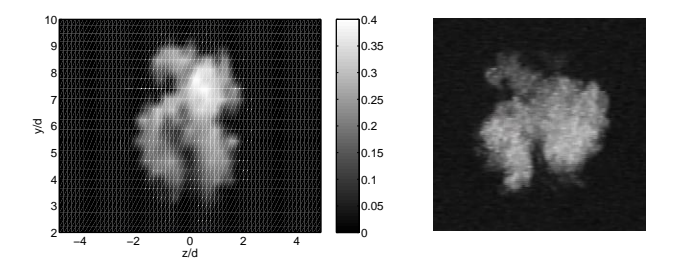


Figure 1.3. Instantaneous profiles of scalar concentration in unforced jet in crossflow at x/d = 3 from simulations (left) and experiments (right).

is evident in flow visualizations of the instantaneous scalar fields of the unforced jet in a cross-plane at $x/D_j = 3$ (figure 1.3).

The scalar fluctuations are largest near the end of the jet's potential core and along the top edge of the jet (figure 1.2). The fluctuations along the top edge of the jet correspond to the passage of coherent packets of jet fluid which result from the rollup of structures associated with the jet shear layer. For a range of frequencies similar to but lower than those for round jets, forcing has a substantial impact on the structure and mixing of the jet. Forcing in the frequency range $St_d = 0.1$ –0.26 leads to increased spreading of the scalar in the wall-normal direction and greater penetration into the crossflow. In these cases, the mean scalar profiles in a y-z slice are qualitatively different from the unforced case, appearing pinched in the center with legs of fluid stretched below. Fluctuations at the upper edge of the jet are enhanced by the forcing which excites the Kelvin-Helmholtz rollup. Forcing at higher frequencies results in a jet



Figure 1.4. Flow visualization from experiments of instantaneous scalar concentration in an x-y plane through the jet centerline for the unforced jet in crossflow (left) and the jet in crossflow forced at $St_d = 0.08$ (center) and $St_d = 0.1875$ (right)

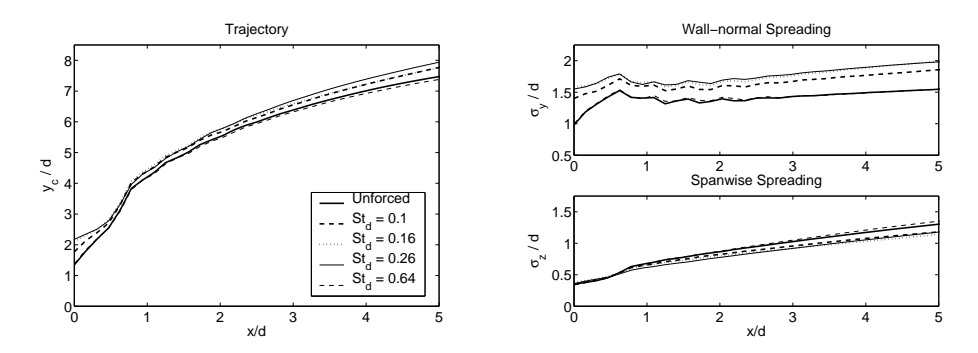
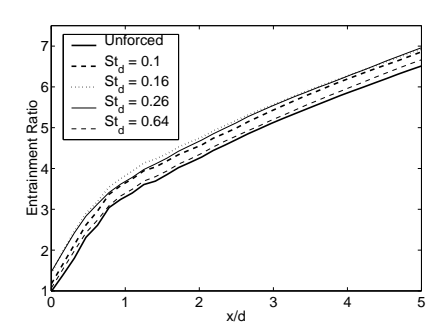


Figure 1.5. Comparison of the trajectory (left) and spreading (right) of the forced and unforced jets in crossflow.

which closely resembles the unforced jet in a time-averaged sense, as in (Schuller et al., 1999; Eroglu and Breidenthal, 2001). However, forcing at the lower frequencies ($St_d=0.1$ –0.26) results in increased energy far away from the jet exit in these lower frequencies, providing an excitable band of frequencies which are beneficial for mixing.

The penetration and spreading of the jet fluid may be characterized by the first and second moments of the mean scalar profiles. The trajectory y_c/d of the jet as a function of the downstream distance x/d is displayed in figure 1.5. With the exception of the highest forcing frequency considered here ($St_d = 0.64$), the forced jets show a slight increase in penetration relative to the unforced jet. The second moment of the scalar profile in the wall-normal and spanwise direction indicates the spreading of the jet in these directions. Forcing also leads to greater spreading of the jet in the wall-normal direction, up to an increase of 30% relative to the unforced jet for $St_d = 0.16$ and 0.26, while the spreading in the spanwise direction is slightly smaller in these forced cases with 10% less spreading for $St_d = 0.16$. The mean scalar profiles shown in figure 1.2 — where low frequency forcing results in scalar profiles elongated



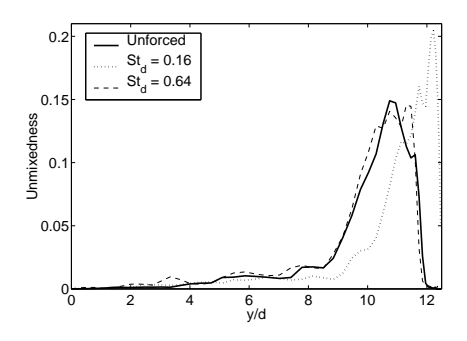


Figure 1.6. Comparison of the entrainment ratio \dot{V}_{jet}/\dot{V}_0 and the level of unmixedness (through the centerline of the jet at x/d=5) of the forced and unforced jets.

in the wall-normal direction — predicted these trends, and these results are confirmed by comparison with the experimental flow visualizations of instantaneous scalar concentration in figure 1.4. In the experiments, the effect of the forcing is more pronounced with greater spreading than in the simulations (as noted before in the discussion of figure 1.1). The excitation of structures in the jet shear layer and the associated increase in intermittency and unsteadiness on the top edge of the jet is shown clearly in the center panel of figure 1.4 (where $St_d = 0.08$).

The jet in crossflow entrains fluid in the same manner as a jet in quiescent fluid — through the structures in the jet shear layer — but also entrains crossflow fluid through the action of the counter-rotating vortex pair (CVP). The entrainment of fluid by the jet may be characterized by the ratio of the volume flux of jet fluid across a given downstream plane $\dot{V}_{jet}(x) = \frac{1}{T} \int_0^T \left(\int_{A_{jet}} u(x,y,z,t) \ dy \ dz \right) dt$ to the volume flux at the jet exit \dot{V}_0 , where the jet fluid is identified by a scalar concentration above 0.01 (Yuan and Street, 1998). (The scalar concentration is one at the jet exit and zero in the crossflow fluid.) The jets forced at lower frequencies ($St_d=0.1,\,0.16,\,0.26$) display enhanced entrainment relative to the unforced jet, entraining more fluid near the jet exit and continuing to entrain fluid downstream at the same rate as the unforced jet.

The level of intermittency and unsteadiness associated with the forcing can be quantified using the 'unmixedness' or 'intensity of segregation' (Danckwerts, 1952; Dimotakis and Miller, 1990). The unmixedness $\Xi = \overline{c'^2}/\overline{c}(1-\overline{c})$ is maximized (with a value of 1) at a point where equal parcels of purely jet and purely crossflow fluid pass. In figure 1.6, the profile of unmixedness in the wall-normal direction at x/d=5 is shown for the unforced jet and the forced jet with $St_d=0.16$ and 0.64. The excitation of the jet shear layer structures leads to increased unmixed-

REFERENCES 9

ness near the top edge of the $St_d = 0.16$ jet (also seen experimentally in the center panel of figure 1.4 where $St_d = 0.08$).

3. Discussion and Conclusions

Unsteady forcing in the appropriate frequency range can have a substantial impact on the structure of and mixing by the jet in crossflow. We have simulated the jet in crossflow to examine the response of the jet to sinusoidal forcing at a variety of frequencies in the range $St_d =$ 0.1–0.64. The range of forcing frequencies was chosen to enable excitation of a variety of coherent structures in the flow, including the "near" field unsteady jet shear layer structures (where most prior studies have focused) as well as "far" field unsteady counter rotating vortex pair dynamics. Both the simulations and experiments indicate that the effect of forcing on the downstream jet mixing is most substantial in the range $St_d = 0.1$ –0.26, where increased spreading, penetration and entrainment is found. The appropriate metric for mixing in the jets in crossflow is an open question and is by no means sufficiently addressed using traditional time-averaged measures (e.g. jet spread). Increased spreading and entrainment often comes at the expense of increased unsteadiness and intermittency in the jet. The acceptability of this unsteadiness is primarily dependent on the timescale associated with the unsteadiness. In a combustion product cooling application, for example, unsteadiness at timescales much faster than the characteristic convection times for heated products traveling past the combustor exit or the heating/cooling timescales of a material subjected to thermal fluctuations (e.g. a turbine blade) may not result in substantial thermal cycling fatigue. However, slower timescales could lead to substantial cycling and fatigue, even for lower time-averaged thermal stresses. Careful interpretation may lead to greater understanding of the importance of unsteadiness and the potential for increased mixing by forced jets in crossflow.

Acknowledgments

The authors would like to thank Dr. Andrzej Banaszuk for his support and for encouraging us to undertake this effort, Drs. Dave Licsinsky, Igor Mezic and Jeff Cohen for fruitful discussions and comments, and Mr. Bruce True for assistance with the experiments. This work was supported in part by internal funding from the United Technologies Research Center and in part by the Air Force Office of Scientific Research through contract no. F49620-01-C-0021 and F49620-01-1-0048. This work was initiated while the first author was a postdoctoral researcher at the University of California, San Diego.

References

- T. J. Anderson, W. Proscia and J. M. Cohen (2001). Modulation of a liquid-fuel jet in an unsteady cross-flow. In *Proc. ASME Turbo Expo* '01. New Orleans, Louisiana, June 2001, paper no. 2001–GT–0048.
- S. C. Crow and F. H. Champagne (1971). Orderly structure in jet turbulence. J. Fluid Mech., 48:547–591.
- P. V. Danckwerts (1952). The definition and measurement of some characteristics of mixtures. Appl. Sci. Res., Sec. A, 3:279–296.
- P. E. Dimotakis and P. L. Miller (1990). Some consequences of the boundedness of scalar fluctuations. *Phys. Fluids A*, 2(11):1919–1921.
- A. Eroglu and R. E. Breidenthal (2001). Structure, penetration, and mixing of pulsed jets in crossflow. AIAA J., 39(3):417–423.
- R. M. Kelso, T. T. Lim and A. E. Perry (1996). An experimental study of round jets in a cross-flow. *J. Fluid Mech.*, 306:111–144.
- B. P. Leonard (1988). Simple high accuracy resolution program for convective modeling of discontinuities. *Int. J. Numer. Meth. Fl.*, 8:1291–1318.
- R. T. M'Closkey, J. M. King, L. Cortelezzi and A. R. Karagozian (2001). The actively controlled jet in crossflow. *J. Fluid Mech.* submitted.
- S. Narayanan, P. Barooah and J. M. Cohen (2002). Experimental study of the coherent structure dynamics & control of an isolated jet in cross flow. In *Proc.* 40th AIAA Aerosp. Sci. Mtg. Reno, Nevada, Jan. 2002.
- J. Nordström, N. Nordin and D. Henningson (1999). The fringe region technique and the Fourier method used in the direct numerical simulation of spatially evolving viscous flows. SIAM J. Sci. Comput., 20(4):1365–1393.
- T. Schuller, J. King, A. Majamaki and A. R. Karagozian (1999). An experimental study of acoustically controlled gas jets in crossflow. *Bull. Amer. Phys. Soc.*, 44(8):111.
- S. H. Smith and M. G. Mungal (1998). Mixing, structure and scaling of the jet in crossflow. *J. Fluid Mech.*, 357:83–122.
- P. J. Vermeulen, C. F. Chin and W. K. Yu (1990). Mixing of an acoustically pulsed air jet with a confined cross-flow. *J. Propul. Power*, 6(6):777–783.
- P. J. Vermeulen, P. Rainville and V. Ramesh (1992). Measurements of the entrainment coefficient of acoustically pulsed axisymmetric free air jets. J. Eng. Gas Turb. Power, 114:409–415.
- L. L. Yuan and R. L. Street (1998). Trajectory and entrainment of a round jet in crossflow. *Phys. Fluids*, 10(9):2323–2335.